AIP | Review of Scientific Instruments

Thrust stand for ground tests of solid propellant microthrusters

S. Orieux, C. Rossi, and D. Estève

Citation: Review of Scientific Instruments **73**, 2694 (2002); doi: 10.1063/1.1483901
View online: http://dx.doi.org/10.1063/1.1483901
View Table of Contents: http://scitation.aip.org/content/aip/journal/rsi/73/7?ver=pdfcov
Published by the AIP Publishing

Thrust stand for ground tests of solid propellant microthrusters

S. Orieux
LAAS-CNRS, 7 Ave du Colonel Roche, 31077 Toulouse Cedex 4, France
and CNES, 18 Ave Edouard Belin, 31501 Toulouse Cedex 4, France

C. Rossi and D. Estève
LAAS-CNRS, 7 Ave du Colonel Roche, 31077 Toulouse Cedex 4, France

(Received 26 February 2002; accepted for publication 8 April 2002)

A pendulum type balance has been designed and fabricated to characterize solid propellant microthrusters. The thrust measurement system mainly consists of a rigid arm rotating freely around a pivot and a feedback control loop. The deflection of the arm produced by the applied thrust is detected using a high frequency transmitter and an antenna. The principle of the measurement is to compensate exactly the thrust force applied to the pendulum by injecting a current in a coil. The measurement of this current gives a perfect image of the thrust force. This article presents the design and performances of the balance. The thrust force measurement sensitivity is 25 μN and the system bandwidth is 40 Hz. Using this balance, single cylindrical thrusters have been characterized. The results gave less than a 1% error between experiment and theoretical evaluation. © *2002 American Institute of Physics.* [DOI: 10.1063/1.1483901]

I. INTRODUCTION

With the miniaturization of space, micropropulsion modules are required to produce very small (below the Newton) and highly accurate forces for stabilization, pointing, and station keeping of nanosatellites. The degree of force impulse precision, the level of thrust, and the weight and space requirements cannot be met with conventional propulsion systems. As a result, over the last decade, micropropulsion has been an active field of research[1–7] and miniaturization of conventional thrusters have been actively investigated from a technological point of view. In this context solid propellant thrusters are good candidates for low thrust impulse.[8,9] One key point to fully validate the solid propellant micropropulsion technology is the accurate characterization of microthrust force. Solid propellant micro thrusters (μSPT) are chemical propulsion devices that use the chemical energy stored in a propellant substance to produce thrust by accelerating the ejected gas stream through a nozzle. They consist of a propellant tank that contains solid fuel, an ignition part made up of an electrical resistor, and a converging diverging part to accelerate the gas stream.[7] Typical μSPT are expected to deliver 300 μN–30 mN during a few tens to hundreds of milliseconds. Solid propellant technology has now reached a good level of maturity. An important step is now is to have accurate thrust measurement capable of fully validating the technology, the propellant, and theoretical models.

II. PURPOSE OF THE THRUST STAND DEVELOPMENT

The aim of the study is not only to have experimental access to the μSPT impulse but also to set up a means of characterization of propellant properties, thruster material, and geometry. The main goal is to validate our predictive models.[10,11] The physics involved in the combustion of composite propellant has often been studied by several groups for ballistic purposes. At the millimeter scale and at low functioning pressure (<10 bars), in systems where thermal losses by convection are significant, many propellant properties are unknown. The burning rate is one of the most important properties for solid rocket designers. Ideally solid fuel burns normal to the burning surface. The linear burn rate is expressed as a function of the burning pressure as follows: $r = aP^n + b$. This relation is empirical and usually accurate over a local pressure range. Coefficients a, b, and especially n are important for the designer. For example, propellants with a high n exponent are unstable at high pressure and can explode when pressurized. The second important parameter at the millimeter scale is the convection coefficient (h) that determines the heat exchanged between gas and rocket walls. The only way in which h and r can be accessed is by experiment. To do so it is important not only to measure accurately the mean force level but also to have the instantaneous thrust. Time resolution must allow determination of the influence of pressure on the combustion rate. Sensitivity and

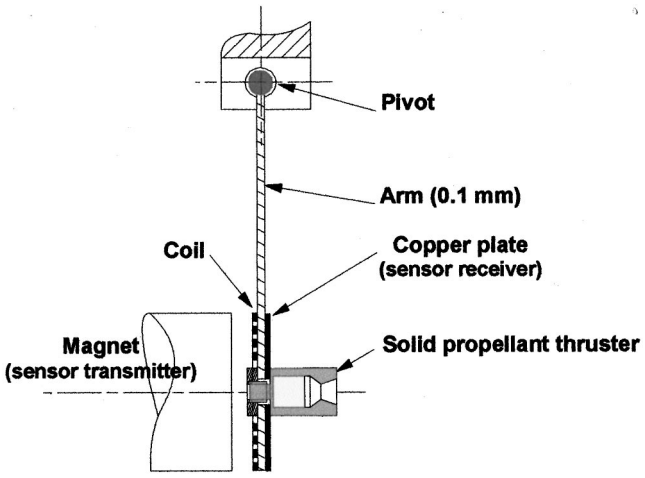

FIG. 1. Schematic view of the thrust stand.

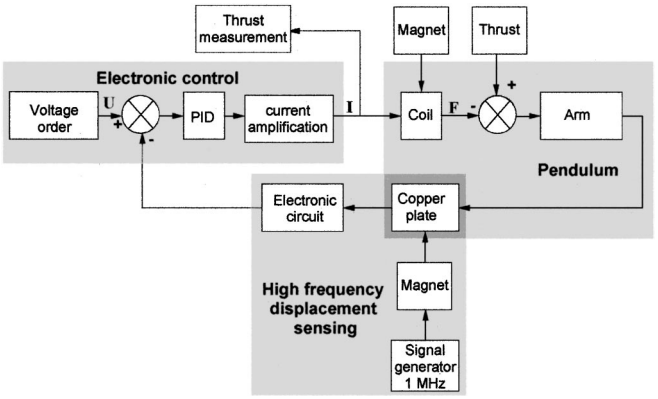

FIG. 2. Block diagram of pendulum and closed loop control.

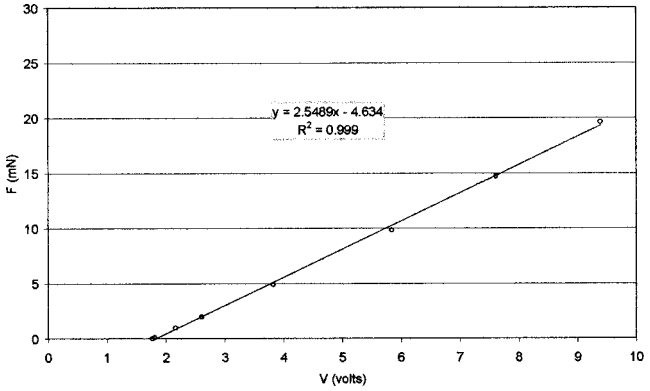

FIG. 3. Thrust stand calibration graph.

time resolution are key elements in our thrust stand design. Using theoretical results,[10] the thrust balance is designed for an operating range of 300 μN–30 mN with a resolution of 10% full scale. The thrust stand system bandwidth requirement is 10 Hz minimum, keeping in mind that the higher the natural frequency is the better the likelihood that the results obtained will be precise. After the state of the art in microforce characterization, this article describes a new thrust stand designed and developed at LAAS-CNRS for μSPT investigation purposes. Typical thrust pulse of 0.4 mN has been measured over a few seconds. Design objectives for the thrust stand are discussed and hardware and calibration results are presented. No systematic characterization is given.

III. STATE OF THE ART

A. Steady-state microthrust measurement

Measuring a force of the order of the Newton is common and many commercially available force sensors can be used. When the thrust level decreases to the milli-Newton, specific methods and equipments are needed to detect it accurately. With the growing miniaturization trend in propulsion field, various teams have been confronted to the characterization of micro- and milli-Newton thrust with the main purpose of measuring steady-state microthrust for electrical thruster. Two types of systems can be found in the literature:

(1) torsion balance with optical readout or accelerometer sensing due to the simplicity and the low sensitivity to vibration.

(2) pendulum type thrust stand. The systems are based on the measurement of the deflection of a beam or a rigid pendulum submitted to the thrust to be measured. For this method, the restoring force is produced by the gravity.[11–14] The sensing element used to measure the beam displacement can be the inductive proximetry probe, an accelerometer, a linear voltage differential transformer, a capacitor system, or an optical angular system. In some cases, the pendulum exhibits an important inertia and is damped electromagnetically.

Typically, the resolution of static thrust balance can reach 0.1 μN. However, all of them present a very low natural frequency (0.1–1 Hz) making them unsuitable for dynamic measurement.

B. Thrust impulse measurement

Impulse measurements differ greatly from conventional steady-state measurements. A large part of the pulse is a transient force which is fast occurring and therefore difficult to measure. The difficulty when designing low thrust and dynamic measurement system is the dilemma met between sensitivity and bandwidth: to obtain a high natural frequency system, one must stiffen the mechanical part that causes a decrease in thrust measurement sensitivity. That must then be compensated by the use of a highly sensitive sensing element. Generally, dynamic force measurement systems aim to find a good compromise between measurement sensitivity and time resolution. Among the dynamic measurement systems found in the literature, none is well suited for transient force measurement. Three dynamic thrust stands have been developed and published for pulsed plasma thruster characterization: Haag[5] developed a torsional type thrust stand to test pulsed plasma thrusters. Momentum per pulse is determined strictly as a function of thrust stand deflection, spring stiffness, and natural frequency. Combin *et al.*[15] designed a balance based on the measurement of the dynamic response of a swinging arm using a two-sensor laser interferometer. Willmes *et al.* has developed an inverted pendulum thrust stand to characterize the pulsed plasma thruster. The thrust stand also contains a proportional-integral-derivative controller for feedback control. Due to the low natural frequency of the system, only average thrust is measured.

These three systems are well suited for a pulsed plasma thruster fired at 2 Hz. For both systems, the bandwidth is typically around the Hz level, which is insufficient for SPT needs.[16–23]

IV. PENDULUM TYPE THRUST STAND AND PRINCIPLE OF OPERATION

The thrust stand is schematically given in Fig. 1. It consists of a thin and rigid arm (100 μm thick) rotating freely around a pivot. The thruster is mounted at the end of the arm, 4 cm from the pivot. On the opposite face of the arm and aligned with the point of thrust application, a coil is deposited. The thrust stand is fixed on a marble block to minimize vibration disturbances during measurements.

The coil is immersed in the magnetic induction field produced by the permanent magnet. When the thrust force is

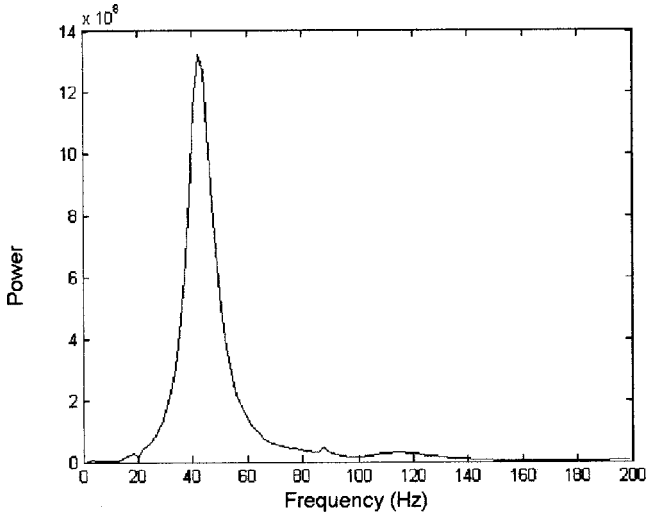

FIG. 4. Frequency spectra of thrust stand (without the 984 mg mass).

applied the pendulum rotates around the pivot axis. A displacement sensor feeds a voltage to the electronic control, which increases the current in the coil and thus the restoring force until the reference position of the pendulum. The reference position is obtained through the voltage order U (see Fig. 2), to keep the arm in a vertical position when the thruster is changed. A high frequency transmitter and an antenna, respectively, a magnet and copper plate, are displacement sensors. The distance between magnet and copper plate modulates the amplitude of the high frequency signal. Then, the signal received by the copper plate is rectified and amplified so as to be compared to the voltage order U. A feedback control is obtained with a (proportional integral derivative) circuit. Measurement of the equilibrium force equal to the thrust is obtained by measuring the electric current I. Figure 2 is a block diagram of the complete thrust stand system.

V. CALIBRATION

For static calibration purposes, the pendulum is laid horizontally. Calibrated masses from 1 mg (10 μN) to 2 g (20 mN) are placed coincident with the thrust axis. As each mass was removed, the thrust signal dropped to zero. No hysteresis was observed. Figure 3 shows the calibration curve showing a good linearity. The entire loop gain is 2.549 mN/V and the sensitivity is 25 μN.

To determine the natural frequency of the thrust stand, a force step is applied to the arm. The natural oscillations of the thrust stand last less than 1 s providing an accurate signal in which harmonic motion can be observed. The curve in Fig. 4 gives the frequency spectra for the thrust stand with a thruster loaded on it. The natural frequency of the system is 42 Hz.

VI. TEST WITH CYLINDRICAL SOLID PROPELLANT THRUSTER

The thrust stand has been validated using a 4 mm diam cylindrical thruster. Cylindrical thrusters have been selected for their reproducibility and rapidity for the fabrication and propellant feeding. Numerous samples were tested for thrust stand validation.

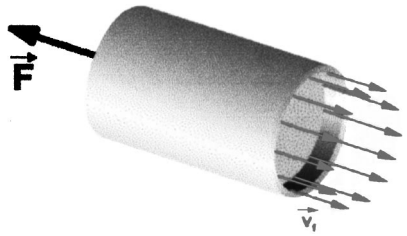

FIG. 5. Characteristics in a cylindrical thruster.

A. Theoretical thrust evaluation

The thrust force F of a particular thruster can be derived from the mass flow rate ($\dot{m}$) of the propellant times the exhaust velocity V_s, added to the thrust due to the pressure against the exhaust area A_s. Assuming an uniform axial velocity that remains constant across the flow area, the thrust force can be expressed as follows:

$$F = \dot{m} V_s + (P_{\text{ext}} - P_s) \times A_s . \tag{1}$$

As the gas exhausts at subsonic velocity, there exists a continuity of pressure along the thruster axis at the exit. Thus the chamber pressure and exhaust pressure are equal to atmospheric pressure:

$$P_s = P_{\text{atm}} . \tag{2}$$

Assuming the gas is perfect, the state equation gives the volumic mass:

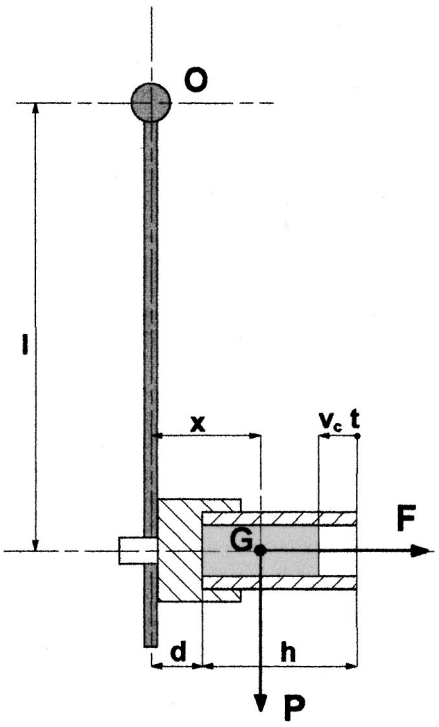

FIG. 6. Schematic view.

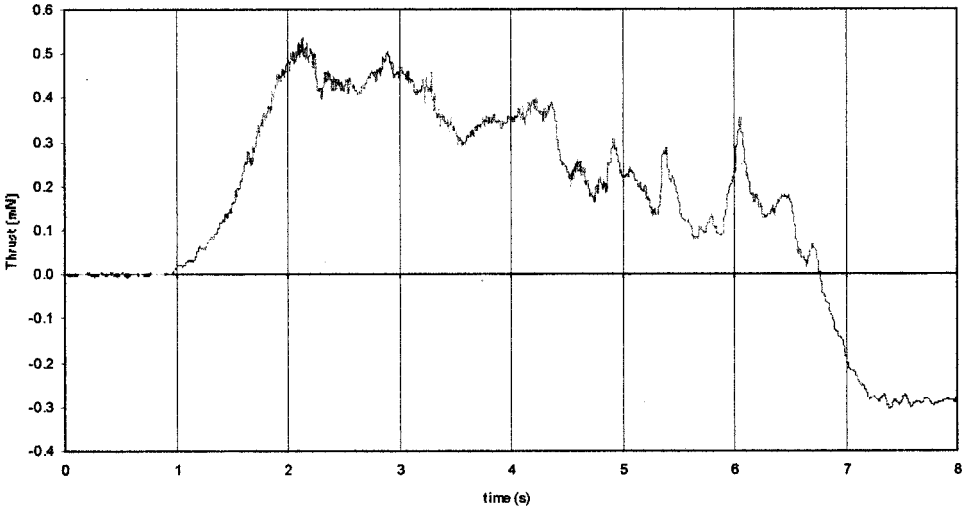

FIG. 7. Output signal after filtering with the Butterworth filter.

$$\rho_s = \frac{P_s}{rT_s}. \tag{3}$$

From the equation of energy conservation, the temperature of the gas can be computed in the following manner:

$$T_s = \frac{h_c}{c_p}. \tag{4}$$

Under steady-state conditions, momentum is also conserved:

$$\rho_s A_s v_s = v_c \rho_p A_s. \tag{5}$$

From Eqs. (1), (2) (3), (4), and (5), the thrust relation becomes

$$F = \frac{rA_s T_s v_c^2 \rho_p^2}{P_{\text{atm}}}.$$

We have calculated theoretical thrust for thruster containing glycidyle azide polymer propellant. It is equal to 0.494 mN.

B. Thrust stand validation

Cylindrical thrusters were filled with propellant and placed on the arm. Combustion ignition was performed with a laser. The laser is triggered as the thrust measurement begins. Signal acquisition is made via a PC using a National Instrument acquisition card (NI 6052 E) sampling at 300 kHz. The output signal is then filtered with a Butterworth type filter (order 6) with a 100 Hz cut frequency.

Ignition occurred 1 s after the laser was on. The combustion lasted 7 s for a 10 mm long thruster, giving a velocity of 1.6 mm/s at the atmospheric pressure. When the combustion finished, the thrust signal dropped to a level lower than the initial value. The difference is 0.28 mN, due to the thruster mass variation during the propellant consumption that creates a torque (Fig. 5).

The torque created by the thruster weight has already been calculated and is compensated for by the feedback control system. The torque created by the mass loss during combustion can be calculated easily as follows.

As shown in Fig. 6, the center of gravity is expressed in the following manner:

$$x = d + \frac{h - v_c t}{2}.$$

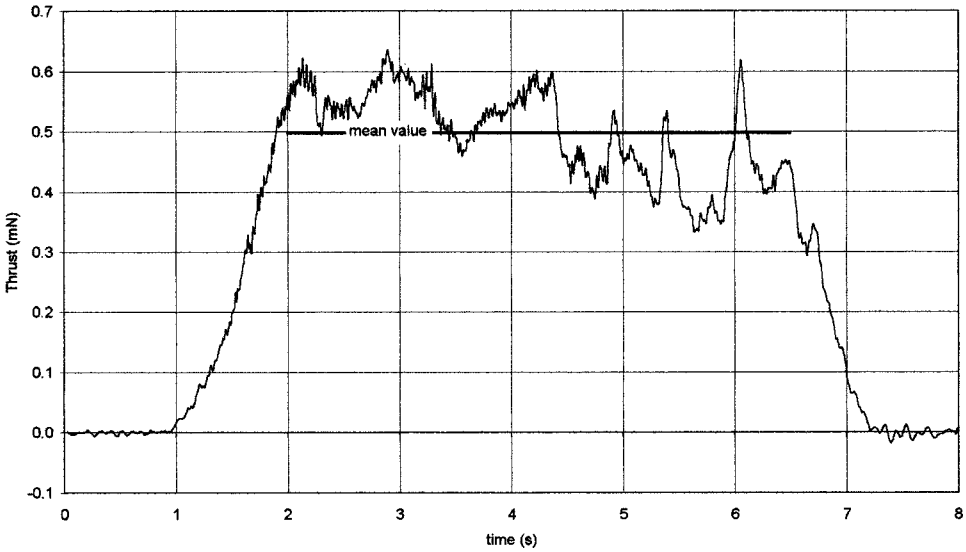

FIG. 8. Experimental and corrected thrust curve for a 4 mm diam cylindrical tube.

The thruster weight is expressed as follows: $P=mg=\rho Vg=\rho(h-v_c t)A_s g$.

Force due to the variation of propellant mass ($F_{\Delta m}$) during combustion is given by the following analytical expression:

$$F_{\Delta m}=\frac{x}{l}P=\frac{2d(h-v_c t)+1}{2l}A_s \rho g.$$

By mathematically removing $F_{\Delta m}$ from the measured thrust force (Fig. 7), the corrected curve can be plotted as shown in Fig. 8. Average measured thrust (without transient phenomena, ignition and end burning) is 0.497 mN (0.494 mN theoretically).

Some improvements are still needed and will be introduced in the coming months. The mechanical pivot will be improved to minimize friction forces. The closed loop control will also be improved to increase stability.

ACKNOWLEDGMENTS

This work has been supported by the European Commission within the project ''Micropyros'' (IST-99 29047). We also acknowledge the French National Center for Spatial Studies (CNES) for additional funded support. The authors thank Henry Bertrand from Valcap for his active participation in this project especially in the electronic design and P. Menini and D. Lagrange for their expertise.

[1] J. Mueller, L. Muller, and T. George, New Technology Report NPO-19926/9525.
[2] D. W. Youngner, S. T. Lu, E. Choueiri, J. B. Neider, R. E. Black, K. J. Graham, D. Fahey, R. Lucus, and X. Zhu, 14th Annual/USU Conference on Small Satellites, 2000.
[3] J. Mueller, I. Chakraborty, S. Vargo, C. Marrese, V. White, D. Bame, R. Reinicke, and J. Holzinger, IEEE Aerospace Conference, Big Sky, Montana, 1999.
[4] X. Ye, F. Tang, H. Ding, and Z. Zhou, Sens. Actuators A **89**, 159 (2001).
[5] E. V. Murkerjee, A. P Wallace, K. Y. Yan, D. W. Howard, R. L. Smith, and S. D. Collins, Sens. Actuators A **83**, 231 (2000).
[6] A. P. London, A. A Ayon, A. H. Epstein, S. M. Spearing. T. Harrison, Y. Peles, and J. L. Kerrebrock, Sens. Actuator A **92**, 2997 (2001).
[7] C. Rossi, T. DoConto, D. Estève, and B. Larangot, Smart Mater. Struct. **10**, 1156 (2001).
[8] H. Helvejian, *Microengineering Aerospace Systems* (AIAA, 1999).
[9] W. A. de Groot, Propulsion Options for Primary Thrust and Attitude Control of Microspacecraft, NASA/CR-1998-206608.
[10] S. Orieux, C. Rossi, and D. Estève, Compact model based on a lumped parameter approach for the prediction of solid propellant micro rocket performance, LAAS Report No. 01403.
[11] A. Sasoh and Y. Arakawa, Rev. Sci. Instrum. **64**, 719 (1993).
[12] J. Bonnet, J. P. Marque, and M. Ory, Third International Conference Spacecraft Propulsion, October 2000, Cannes, France.
[13] T. Haag, Rev. Sci. Instrum. **68**, 2060 (1997).
[14] A. Franks, M. Luty, C. J. Robbie, and M. Stedman, Nanotechnology **9**, 61 (1998).
[15] E. A. Combin, J. Z. Ziemer, E. Y. Choueiri, and R. G. Jahn, Rev. Sci. Instrum. **68**, 2339 (1997).
[16] C. Rossi, M. Djafari Rouhani, and D. Estève, Sens. Actuators A **87**, 96 (2000).
[17] F. Paolucci, L. d'Agostino, and S. Burgoni, Proceedings of the Second European Spacecraft Propulsion Conference, 1997 (ESA SP-398, 1997), pp. 465–472.
[18] T. W. Haag, Rev. Sci. Instrum. **62**, 1186 (1991).
[19] L.I. Winkler, Rev. Sci. Instrum. **57**, 3019 (1986).
[20] M. Stedman, A. Franks, M. Luty, and C. J. Robbie, Proceedings of the Second European Spacecraft Propulsion Conference, 1997 (ESA SP-398, 1997), pp. 461–464.
[21] A. Sasoh and Y. Arakawa, Rev. Sci. Instrum. **64**, 719 (1993).
[22] Y. Katagiri and K. Itao, Appl. Opt. **37**, 7193 (1998).
[23] G. F. Willmes and R. L. Burton, J. Propul. Power **15**, 440 (1999).